Received 11/21/05
MSHA/OSRV

MICROSCOPE Vol 51:3 121-140 (2003)

Morphological and Optical Characterization of Amphiboles from Libby, Montana U.S.A. by Spindle Stage Assisted - Polarized Light Microscopy

Brittany M. Brown and Mickey E. Gunter
Department of Geological Sciences, University of Idaho*

KEYWORDS

Asbestos, polarized light microscopy, PLM, spindle stage, Libby, Montana, tremolite, amphibole, extinction angle, aspect ratio

INTRODUCTION

Asbestos has been a major health concern in the United States since the 1960s (1). Since then, much has been learned about common asbestos minerals and presented in several works (2-4). For instance, we know that the most commonly used asbestos variety, chrysotile - a serpentine mineral, appears to be less harmful than the more rarely used amphibole asbestos varieties (5-7). Also, several studies have shown that the fibrous variety of tremolite, i.e., tremolite-asbestos may be the most harmful of the amphibole minerals (8-12). The creation of regulatory agencies, like the Occupational Safety and Health Administration (OSHA) in 1970, and the regulations they have developed since 1972, have greatly reduced the risk of asbestos-related diseases to the point where, over the past decade, asbestos has fallen off the front page of the newspapers and out of the minds of the general public. This changed on November 18, 1999, when the Seattle Post-Intelligencer published an article about asbestos-related diseases of former miners in Libby, Montana (13). The miners worked in the world's largest vermiculite mine owned by W.R. Grace from 1963 to its closure in 1990. It had previously been owned by Zonolite Corporation with operations since 1923. The vermiculite ore was reported to contain approximately 5% tremolite-asbestos and exposure to this impurity in the ore caused an increase of asbestos-related disease in the miners. This article caught the attention of the United States Environmental Protection Agency (EPA), which arrived on the scene in a few days. Since then, millions of dollars have been spent on remediation in the area and health studies have begun.

Originally, the only amphibole believed to be in the mine in Libby was tremolite, however recent work (14) showed that two samples from the mine are winchite, which is not one of the six regulated asbestos minerals. Gunter et al. (15) confirmed these results using the same set of Libby amphibole samples in this morphological study.

ASBESTOS NOMENCLATURE – DISTINGUISHING AMPHIBOLE FRAGMENTS FROM FIBERS

Although not commonly viewed this way, there are two basic definitions of asbestos; one is physical and the other chemical. As with any definition, problems arise with natural samples based on our limitation to formally describe nature.

The physical definition of asbestos deals with its morphology or shape. Regulatory agencies consider a particle to be asbestos, for counting purposes, if its aspect ratio is 3:1 or greater and the particle is over 5 μm in length (5, 7, 16). This is, of course, very different from the physical characteristics a mineralogist would use – that the particle must have a fibrous form (see reference 19 for an overview of asbestos terms).

The chemical definition of asbestos used by regulatory agencies for identification includes six mineral species. These minerals are chrysotile, crocidolite, amosite, tremolite, actinolite, and anthophyllite (5, 7, 16). Chrysotile is the asbestos form of serpentine, a sheet silicate. The others in this group are all amphiboles. Crocidolite and amosite are asbestiform varieties of the amphibole minerals riebeckite and grunerite, respectively. Thus the names chrysotile, crocidolite, and amosite always denote asbestos minerals, while tremolite, actinolite, and anthophyllite can occur in

* Moscow, Idaho 83844-3022, U.S.A.

AB24-COMM-110-1

either a non-asbestos (non-fibrous) or asbestos (fibrous) form, with the non-asbestos form being much more common in the geological environment.

There has been considerable controversy, for over 20 years, on distinguishing cleavage fragments, or single crystals of amphiboles, from fibers of amphiboles (10, 20-22). The underlying reason is that cleavage fragments, when inhaled, appear to be less harmful than fibers (12, 19, 23). Based on a review of all the existing literature, cleavage fragments of the amphibole minerals were deregulated in 1992 (23). Regulatory agencies simply use the aspect ratio to make the distinction between fragments and fibers, however, as we show in this paper (and has been shown by other researchers: 5, 16, 19, 21), this definition simply does not work. Fibers and fragments possess different physical properties and, as always, the physical properties of a mineral are directly related to its structure.

The structural difference between a fragment and a fiber is that fibers of asbestos are made up of many crystals, i.e. they are polycrystalline. They occur as fiber bundles comprised of individual fibrils, much like a rope is made of many small strands; giving asbestos its incredibly high tensile strength and flexibility (24). And, as Wylie (16) points out, common asbestos fibril sizes range from 500 Å in chrysotile to 6,000 Å in some amphibole-asbestos samples. Fragments, in turn, are single crystals. Thus, any analytical method that could distinguish polycrystalline materials (e.g., intergrown fibers) from a single crystal (e.g., growth or cleavage fragments) would work to distinguish fibers from fragments. This can be determined with polarized light microscopy on particles as small as 1 μm; however, when the particles reach a width and thickness of a few microns certain useful optical properties (i.e., extinction characteristics) become difficult to observe and measure due to lower retardation. In addition, Wylie (21) noted that monoclinic amphiboles (e.g., tremolite and actinolite) yield parallel extinction when they occur as fibers, instead of the expected inclined extinction. While this method works most of the time, it has limitations as discussed herein.

Diffraction methods (X-rays or electrons) can also be used to determine crystallinity i.e., single versus polycrystallinity. Wylie (21) showed that amphibole fibers display a polycrystalline diffraction pattern in the ab-plane. TEM methods have also been used on very small samples. When an amphibole particle is rotated about its c-axis, the electron diffraction patterns remain the same if it is a fiber, but changes if it is a single crystal (19).

Typically, cleavage fragments of amphiboles expose the (110) plane. However, it has been shown by past researchers (25) that single small crystals of amphiboles are flattened on (100); our study confirms this observation. In fact, this study shows that there is a possible relationship between crystal size and (110) or (100) surface development. It has also been shown that amphibole fibers are flattened on (100) (24, 26). Thus, we speculate that it might not be the fibrous form of the amphibole alone that poses the health risk, but the exposed surface, i.e., (110) surfaces may be less harmful than (100) surfaces and perhaps these surfaces, by exposing different planes of atoms in the mineral, may react differently in the human lung. Also, the surface area would be greater for a given volume of material as particle size decreases.

With the recent concerns at Libby, the definition of asbestos by the regulatory agencies comes into question; this should result in changes in regulations. For instance, as outlined in (15), the health risks associated with whatever amphiboles occur at Libby are significant. It appears that, regardless of species type, all amphibole-asbestos should be regulated. This might also extend to all fibrous silicates in general. For instance, erionite, a fibrous zeolite, has been shown to induce mesothelioma in very high amounts in lab animals and been linked to outbreaks of mesothelioma in Turkey (27). The common denominator in most of these health-related mineral problems is fibrous silicates, and perhaps they should all be regulated. However, quartz, which was recently upgraded to a Group 1 human carcinogen, is not fibrous (29). Again, silicates seem to be the common thread (27-32). Clearly this needs to be revised in light of Libby to include, at the least, all amphibole-asbestos. At present, we are left with only the six "asbestos minerals" being regulated.

GOALS OF THE STUDY

In this study we attempted to characterize the shape of particles and classify them as either single crystals, which we termed as fragments, or multiple crystals, which we termed as fibers. As such, photomicrographs of the samples provide a qualitative description. We made thousands of optical measurements on the samples in this study, and quantified these data in a series of descriptive tables. The "Results" and "Discussion" are divided into two distinct but complementary sections: analyses done on grain mounts, which is the common method of characteriz-

ing asbestos particles, and analyses of single particles with the aid of the spindle stage.

One of our goals for examining single particles was to aid in understanding our observations on grain mounts i.e., we could determine the precise extinction angles when the particles were mounted on the spindle stage, and to observe the morphological characteristics of the particles in 3D as compared to 2D in the grain mounts. Other researchers have measured aspect ratios for amphibole particles in grain mounts (e.g., 16-17), but none have done this with the spindle stage. With the spindle stage, the thickness, length and width can be measured so that the volume of a particle can be calculated. Wylie et al. (18) made a similar set of measurements on the thickness of smaller amphibole particles using both an SEM and TEM.

MATERIALS

Three separate samples were chosen for this study: a non-asbestos tremolite from our teaching collection (called UI tremolite herein), a NIST tremolite asbestos standard (NIST asbestos standard #1867), and amphiboles collected from the former vermiculite mine near Libby, Montana by the author (MEG) in October 1999. The UI tremolite sample was selected to represent a non-fibrous amphibole and to obtain data on cleavage fragments. The NIST tremolite was selected for a comparison to the Libby amphiboles. In general, tremolite samples were selected because the amphiboles from Libby had been reported to be tremolite. Since this project started, Wylie and Verkouteren (14) showed this not to be the case; they determined that two samples of Libby amphibole were winchite. Our ongoing research (15) also found the samples to be winchite and richterite. Nevertheless, the tremolite samples chosen for this study were used to compare differences in morphology and optical characteristics to the Libby amphiboles, because no winchite and/or richterite standards exist at this time. However, winchite-asbestos has been shown to occur in nature (33).

The Libby samples were further divided based on occurrence at the mine. Three samples were chosen. One was collected, in place, from one of the mined-out benches (15), called "outcrop" in this work. A second sample was taken from a 2 cm vein of amphibole in the biotite pyroxenite, the rock mined for vermiculite, called "vein" herein. The third was taken from an approximately 20 cm boulder consisting entirely of amphibole, which was resting on the ground in the middle of the abandoned mine, labeled "float."

EXPERIMENTAL METHODS

Two separate optical procedures were used to characterize the three different amphibole samples. One procedure employed a PLM to measure particle dimensions (i.e., length and width by use of a calibrated eyepiece), morphology, and extinction angles to determine if a particle was either a fiber or fragment in grain mounts. The second procedure used the PLM equipped with a spindle stage to measure particle dimensions (i.e., length, width, and thickness with the aid of a Vicker's image splitting eyepiece), morphology, and extinction angles as a function of orientation to determine if a particle was either a fiber or fragment.

Grain mounts were made for each of the samples by placing a small of amount of each on a standard petrographic slide with 1.55 refractive index liquid. This refractive index value was chosen so the particles could be easily seen in plane polarized light. Each sample was prepared as follows. The UI tremolite was crushed and sieved to –60 mesh (250 μm). The NIST tremolite, which was provided from NIST already comminuted, was sieved to –60 mesh (250 μm). The Libby samples were crushed, pulled apart, and sieved to –60 mesh (250 μm). An extra step was added for both the NIST and Libby samples; they were placed in acetone and ultrasonicated to further break the particles apart.

For the spindle stage study, single particles were selected from the same samples as prepared for the grain mounts. These single crystals were attached to a glass fiber with fingernail polish with their long dimension approximately parallel to the fiber and placed on the spindle stage with the aid of a goniometer head (34). By angular adjustments on the goniometer head, each particle was made parallel with the rotation axis of the spindle stage. In this manner, the width and thickness were observed and measured. Additionally, extinction angles were measured on the (hk0) planes, i.e., (100), (010), and (110) or on the planes corresponding to the widest and thinnest portions of the crystals.

RESULTS - GRAIN MOUNTS

Eleven (11) total grain mounts were prepared. One slide for each of the UI tremolite and NIST tremolite was prepared and three slides were prepared for each of the three Libby samples (outcrop, vein, float). On each slide, 100 particles were chosen at random and their width and length were measured. They were classified as either fragment or fiber based on mor-

phological and optical properties (i.e., extinction characteristics) and their extinction angles were measured. Also, each particle was briefly described. It would be impractical to list all of the data, so select photomicrographs (Figures 1-3) and a series of tables (all tables are located in the Appendix, pp. 132-138) are used to summarize it.

Figure 1 shows grain mount photomicrographs of the UI tremolite (Figs. 1A and 1B), the NIST tremolite (Figs. 1C and D), and the Libby amphibole (Figs. 1E and 1F). The photomicrographs in the left column were taken in plane-polarized light, and in the right column the same sample is photographed again but this time in crossed polars. There is a distinct increase in the aspect ratio when comparing the UI tremolite, to the NIST tremolite asbestos, to the Libby amphibole. The circled particles in Figures 1A, 1C, and 1E would be classified as asbestos if based on aspect ratio alone (12:1, 16:1, 30:1, respectively), however, the circled particle in Figure 1A is a cleavage fragment and not asbestos, as is the circled particle in Figure 1C. This distinction is made based on morphology and extinction conditions as shown in the corresponding Figures 1B and 1D.

All of the important characteristics of the particle circled in Figure 1E are difficult to show in two photomicrographs. However, morphologically, the blunt ends would indicate it is a fragment but its curvature would indicate it is a fiber. The particle shows inclined extinction in Figure 1F and it shows complete, sharp extinction as the stage is rotated. For these reasons, this particle is classified as a fragment. If the extinction had not been complete, we would not have classified it as either a fragment or a fiber because it would have showed characteristics of both fibers and fragments.

It is also noteworthy to point out that, for the UI tremolite, most of the particles are visible in both plane polarized and crossed polarized light, while this is not the case for the other two samples. The particles in the UI tremolite sample have a higher retardation because they are lying on (110) while particles in the other two samples more commonly are resting on (100). This phenomenon will be elaborated on in the "Discussion" section.

Table 1 gives the particle count based on width and length. Notice there are 100 particles for the UI tremolite and only 99 particles for the NIST tremolite asbestos; one of the particles in the NIST sample was calcite. For the Libby samples, data from the three slides were combined, yielding a total of 300 particles for each. The Libby outcrop sample had two calcite particles and the Libby vein had one.

Given the length and width data, aspect ratios were calculated for all of the samples. Table 2 lists the percentage of particles with different aspect ratio ranges for the five samples. Also given in Table 2 are the divisions of the particles into three groups: fibers, fragments, and not classified based on morphology. Table 3 merely combines the three Libby samples into one and is similar to Table 2. Table 4 is a summary of the five samples classified based on aspect ratio (Table 4A) and by morphology (Table 4B). Table 5 again lists the five samples, but this time they are broken down on a particle count based on four extinction conditions: 1) "parallel," when the particle exhibited parallel extinction, 2) "inclined," when the particle exhibited inclined extinction, (also included in this column is the average extinction angle and its standard deviation), 3) "isotropic," when the particle exhibited near-zero retardation, and 4) "cannot measure," for particles that never went extinct or had wavy extinction.

RESULTS - SINGLE PARTICLES

In order to characterize the size (i.e., length, width, and thickness), extinction characteristics, and morphology of the three samples in this study; ten (10) particles of the UI non-asbestos tremolite, twenty-five (25) particles of the NIST tremolite, and fifty (50) particles of the Libby vein samples were mounted on glass fibers and observations and measurements were made with the aid of a spindle stage equipped PLM. Tables 6, 7, and 8 list the results for length, width, thickness, aspect ratio (l/w), aspect ratio (l/t), aspect ratio (w/t), the extinction angles (measured on two different planes), and the morphological characterization of these 85 particles. Table 6 lists these results for the UI tremolite sample in two different manners. Table 6A lists measurements for the widest and thinnest directions of the particle. These were obtained by rotating the sample about the spindle axis to find the largest and smallest dimensions. For all of the particles except #4 and #10, these directions do not correspond to the (100) or (010) directions, which is to be expected for an amphibole exhibiting (110) cleavage. Particles #4 and #10 are flattened on (100), which is obvious by the fact that they exhibit parallel extinction. In Table 6B, each particle was rotated so the (100) direction was brought parallel to the stage of the microscope; this is determined by the condition of parallel extinction. Its width and extinction condition were measured on

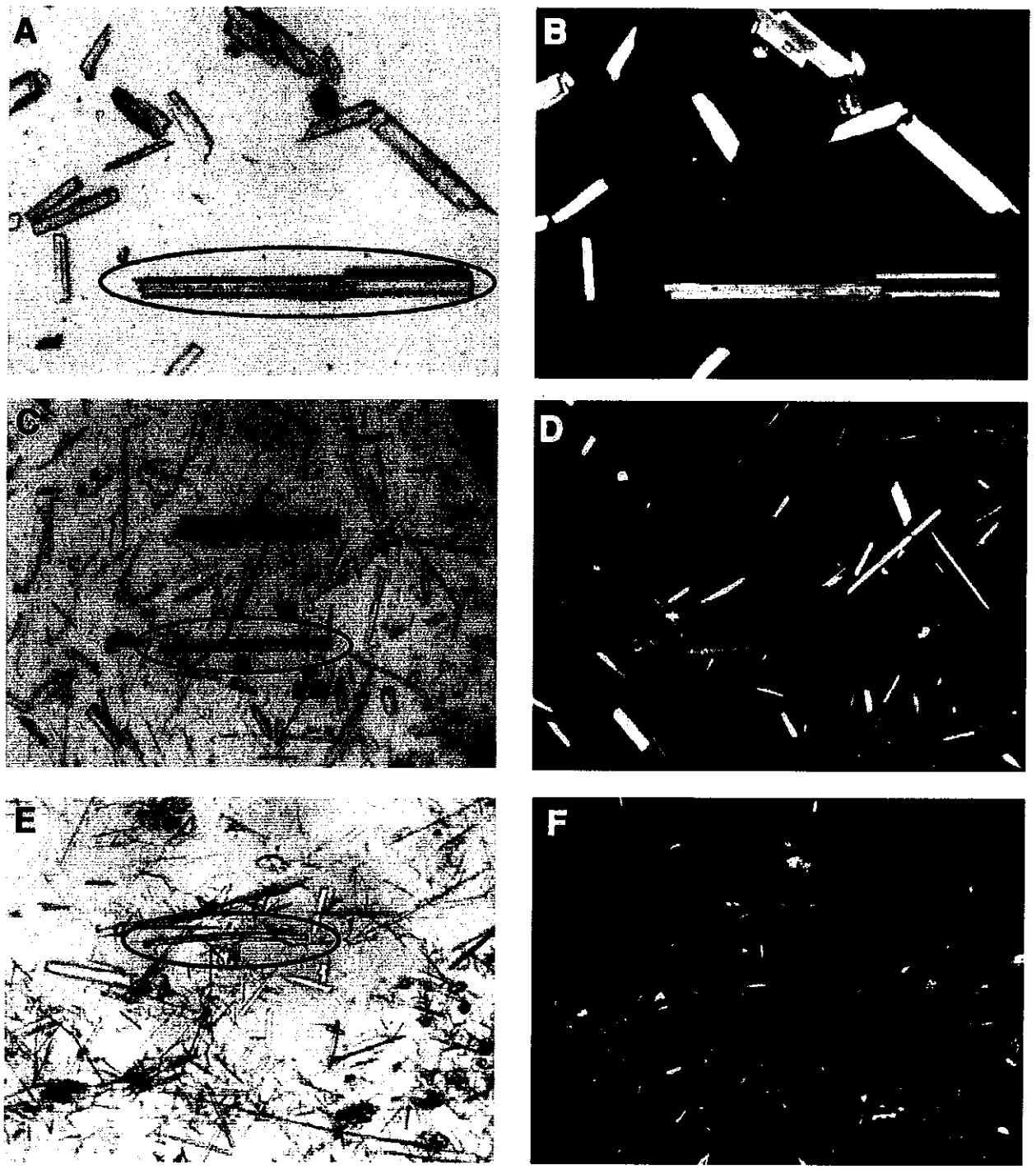

Figure 1: Photomicrographs of UI non-asbestos tremolite (A and B), NIST tremolite asbestos (C and D), and Libby amphibole (E and F). Photographs in left column correspond to those in the right column, with those in the left column taken in plane-polarized light and those in the right column taken in cross-polarized light. Circled minerals are discussed in the text. (Field of view is approximately 500 μm wide; samples are immersed in a 1.55 refractive index liquid.)

(100). The particle was then rotated and its thickness and extinction condition were measured on (010).

Figures 2 and 3 show photomicrographs of differing morphologies of the three samples immersed in a 1.55 refractive index liquid using the spindle stage. The images are of the same particles in the left and right columns, except the crystals have been rotated 90° about the spindle axis. Each particle was attached with fingernail polish (fluid-looking material) onto a glass fiber (the fibers are approximately 100 to 200 μm in diameter). Figure 2A is a photomicrograph of a single UI tremolite particle (particle #9, Table 6) viewed perpendicular to its widest direction; Figure 2B is the same particle as in Figure 2A, except the crystal has been rotated 90° to view it normal to its thinnest direction. Figures 2C to 2H are photomicrographs of the NIST tremolite sample. Figures 2C and 2D are of particle #5, Table 7 and Figures 2E and 2F are of particle #7, Table 7; both of these particles are considered fiber bundles based on their morphology. Figures 2G and 2H are NIST tremolite #21, Table 7 which is considered a fragment based on its morphology.

In Figure 3 are four samples depicting the three differing morphologies encountered in the samples from Libby. Figures 3A and 3B are of particle #7, Table 8, considered a fiber bundle, as is particle #22, Table 8 (Figures 3C and 3D). Figures 3E and 3F are of a particle considered to be a fiber mass (particle #18, Table 8). Lastly, Figures 3G and 3H show a fragment of the Libby amphibole (particle #21, Table 8). It is worth noting the orientations of the three fragments shown in this series of photomicrographs. In Figure 2A, we are looking down on the (110) surface; this is typical of cleavage fragments. In Figures 2G and 3G, we are looking at the (100) surface; this is typical of smaller amphibole crystals, i.e., they are flattened on (100).

DISCUSSION - GRAIN MOUNTS

Based solely on observation of Figure 1, there is an increase in the aspect ratio going from the UI tremolite (Figure 1A) to the NIST tremolite (Figure 1C) to the Libby amphibole (Figure 1E). The data in Tables 1 and 2 quantify this increase in aspect ratios observed in the Figures. Table 2 shows the percent non-asbestos, based on aspect ratio, to be 52% for the UI non-asbestos tremolite and 8% for the NIST tremolite asbestos. For the three Libby samples, these values are 0%, 5.4%, and 8.7% for the outcrop, vein, and float, respectively. Combining the three Libby samples, they would have 5% non-asbestos particles based on aspect ratio. Very different results are obtained basing the asbestos and non-asbestos proportions on morphology. Table 4 summarizes the data for all five samples and classifies each based on both aspect ratio (Table 4A) and morphology (Table 4B). Based on morphology, and mineralogical considerations, the entire UI tremolite sample is non-asbestos, as compared to 52% non-asbestos based on aspect ratios. For the NIST tremolite sample, 52% is non-asbestos based on morphology, while only 8% was non-asbestos based on aspect ratio. Lastly, the combined Libby sample shows the smallest amount of non-asbestos particles based on morphology, 33%, and aspect ratio, 5%. Also, note in Table 4 that we were unable to classify, as either fiber or fragment, approximately 30% of the NIST and Libby samples. Thus, the results based on aspect ratio differ significantly from those based on morphology, especially for the non-asbestos UI tremolite sample.

Our aspect ratio data yield similar results to two other studies. Wylie (35) found that a non-asbestos tremolite had 47% of the particles with an aspect ratio greater than 3 and 3% with an aspect ratio greater than 10, as compared to 48% and 4%, respectively, for the UI tremolite sample.

Basically, there are three types of particles in this study: fibers, cleavage fragments (which exhibit (110) cleavage), and single crystals, which are usually flattened on (100). Observation of extinction conditions has helped past researchers distinguish monoclinic amphibole fibers from cleavage fragments (21); in fact, OSHA mentions this method. The premise for this is that a fiber will show parallel extinction whereas a fragment will show inclined extinction.

Figure 4 shows sketches of monoclinic amphiboles with optical orientations similar to tremolite, winchite, and richterite. The lower illustration in Figure 4A represents an amphibole resting on its (110) cleavage surface. In this orientation, the sample would show inclined extinction; however, this orientation does not represent the true extinction angle (the angle between c and Z) which would be observed when a sample rested, or was viewed, on its (010) surface (lower illustration, Fig. 4B). Parallel extinction can occur because fiber bundles are elongated parallel to the c axis and the individual fiber's a- and b-axes are at random directions to this elongation; thus, the Z direction would average out over many particles to be parallel to the long direction of the fiber. This again means that an asbestos particle is really a polycrystalline material, while a fragment is a single crystal. This difference in crystallinity can be observed optically. However, if a single crystal of a monoclinic amphib-

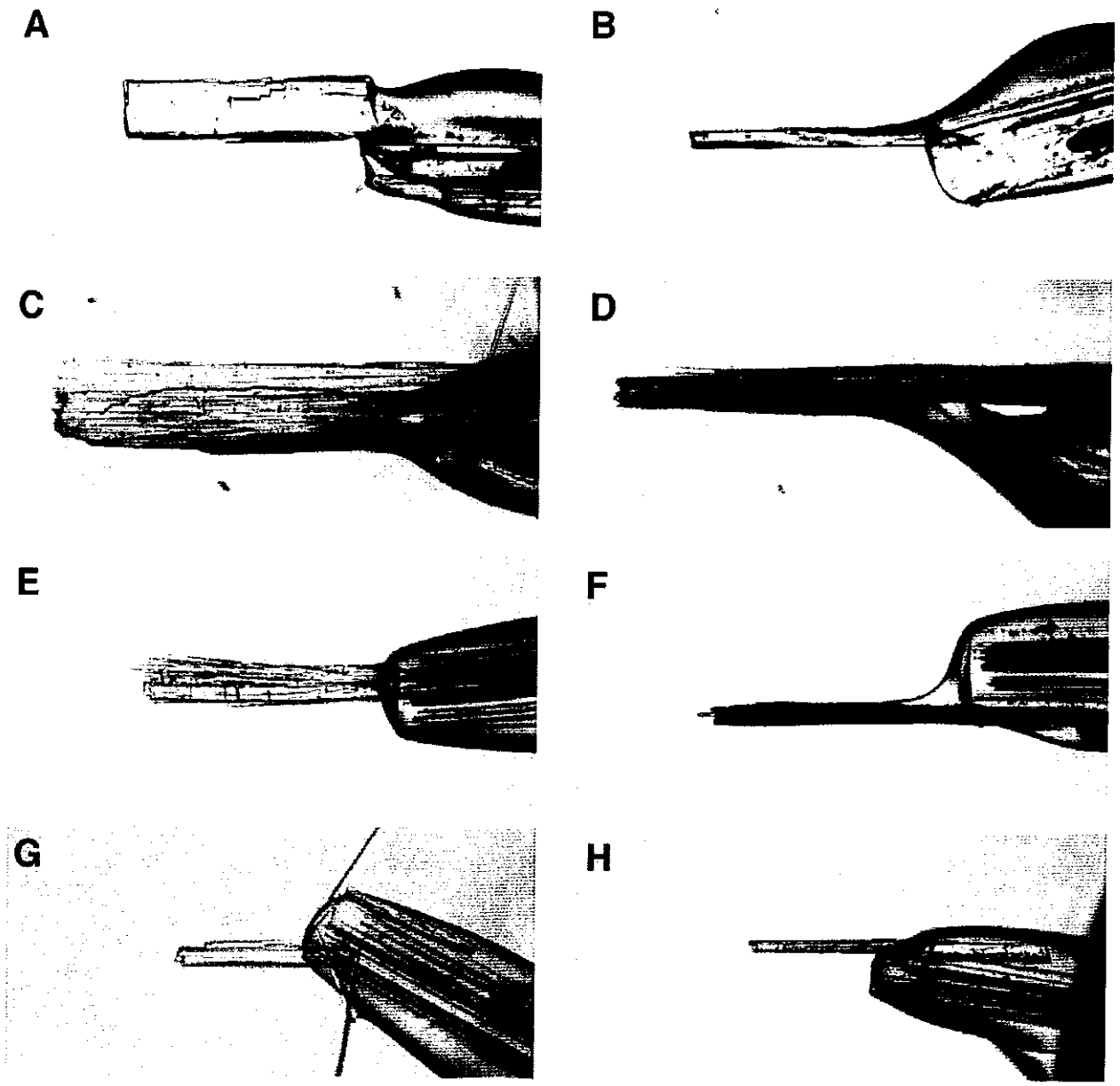

Figure 2. A) Image of UI tremolite #9 fragment (Table 6) viewed perpendicular to its thinnest direction; length is 562 μm; B) Sample in A rotated 90°; C) Image of NIST tremolite #5 fiber bundle (Table 7) viewed perpendicular to its thinnest direction; length is 728 μm; D) Sample in C rotated 90°; E) Image of NIST tremolite #7 fiber bundle (Table 7) viewed perpendicular to its thinnest direction; length is 594 μm; F) Sample in E rotated 90°; G) Image of NIST tremolite #21 fragment (Table 7) viewed perpendicular to its thinnest direction; length is 302 μm; H) Sample in G rotated 90°.

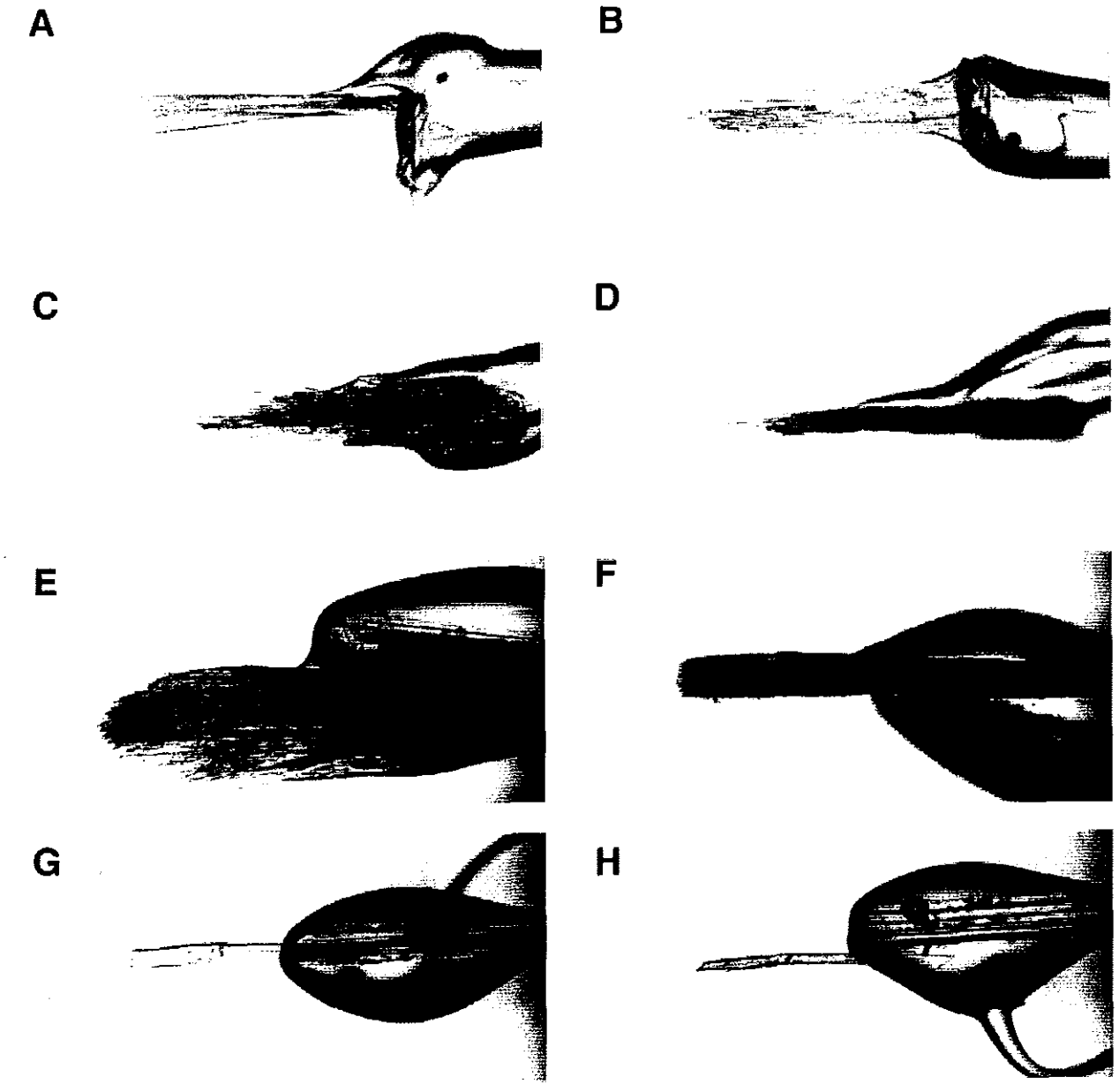

Figure 3. A) Image of Libby #7 fiber bundle (Table 8) viewed perpendicular to its thinnest direction; length is 537 μm; B) Sample in A rotated 90°; C) Image of Libby #22 fiber bundle (Table 8) viewed perpendicular to its thinnest direction; length is 512 μm; D) Sample in C rotated 90°; E) Image of Libby #18 fiber mass (Table 8) viewed perpendicular to its thinnest direction; length is 438μm; F) Sample in E rotated 90°; G) Image of Libby #47 fragment (Table 8) viewed perpendicular to its thinnest direction; length is 375 μm; H) Sample in G rotated 90°.

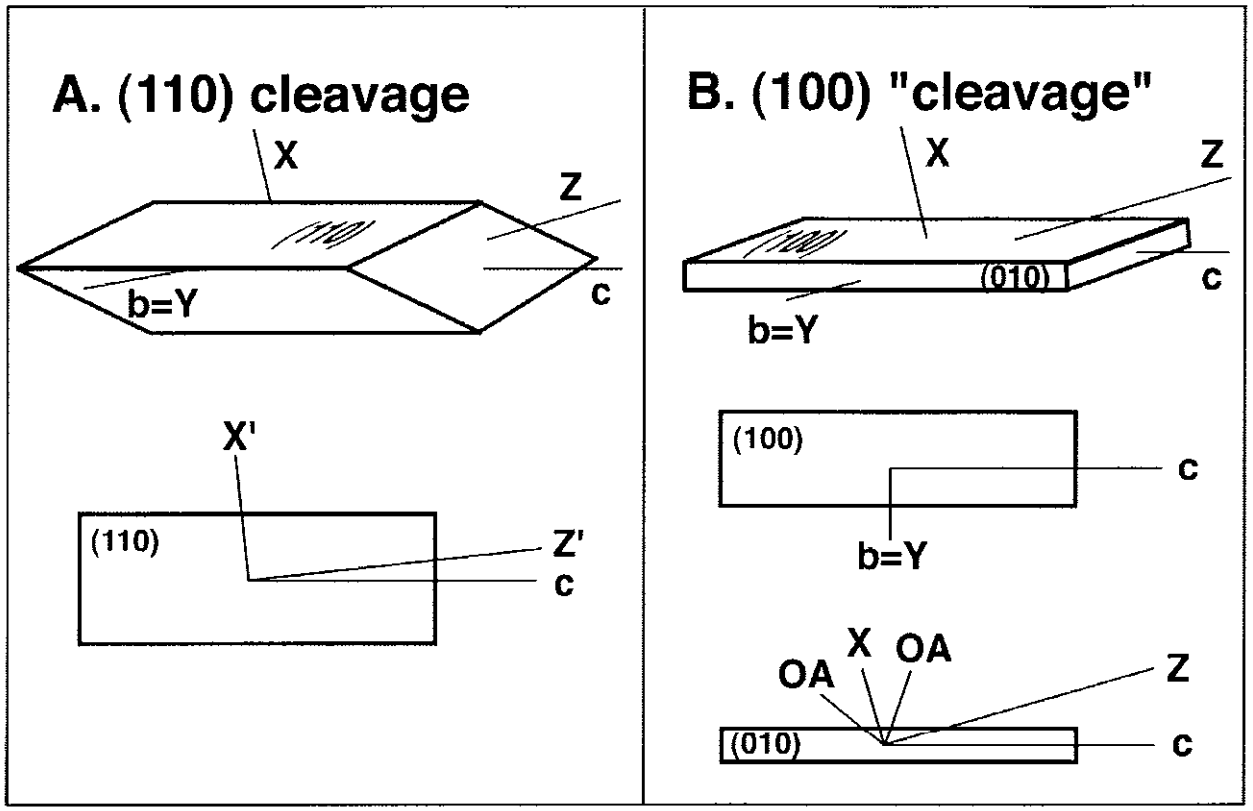

Figure 4. A) Typical cleavage fragment of a monoclinic amphibole (top) showing the (110) cleavage faces, crystallographic axes, and optical vibration directions (indicated by X' and Z'), and a similar crystal (bottom) resting on a (110) cleavage surface. B) A monoclinic amphibole (top) flattened on (100) and elongated along c, a crystal (middle) resting on (100) that would show parallel extinction (middle), and the view (bottom) looking down b on the (010) plane. The optic axes are indicated by OAs.

ole is flattened on (100), it will also show parallel extinction (Fig. 4B). Lastly, extinction positions become increasingly more difficult to observe as the particles become thinner because the retardation decreases.

Compounding this problem, especially for particles (e.g. tremolite and winchite) resting on the (100) surface, is a decrease in the birefringence of that plane based on the optical orientation of the mineral, because a circular section (isotropic view) of the indicatrix is near parallel to the microscope stage (Fig. 4B). Thus, precautions need to be taken when using extinction data for determining fibers vs. fragments. In this study we have measured the extinction angles for the differing directions for all three of our samples, in order to use these data to help interpret which form the samples have.

Su and Bloss (37) give equations for calculating extinction angles for any (hk0) plane in a monoclinic amphibole based on its optical orientation and 2V, and they warn how extinction angles are often misinterpreted. For instance, it is often assumed that the extinction angle increases from zero for a sample resting on (100) to a maximum when the sample rests on (010). This assumption is not always true (i.e., the maximum "extinction" angle may occur on some (hk0) plane other than (010)). Bandli and Gunter (13) have shown that the Libby samples exhibit (100) and (110) faces. Thus, we expect different extinction angles depending on the face the sample rested on.

The circled crystal in Figure 1A, the UI tremolite sample, is resting on (110) and exhibits inclined extinction in Figure 1B. This sample is in the orientation as shown in the bottom sketch in Figure 4A. In this orientation, the sample has an extinction angle of 13°, which is not the true extinction angle (as measured on (010)) of 16°. Table 5 summarizes the extinction data for all the samples in this study. For the UI tremolite, 99 of the particles rested on (110) and yielded

an extinction angle of 13°, while one fragment rested on (100) and gave parallel extinction. For the NIST tremolite sample in Figure 1D (the circled crystal in 1C), the crystal shows inclined extinction indicating that the sample is resting on its (110) surface. Table 5 shows that 15 of the 99 NIST tremolite fragments were in this orientation, while 22 of them showed parallel extinction. Thus, 59% of the NIST fragments with observable extinction rested on (100), while 1% of the UI tremolite fragments were flattened on (100). These particles were fragments even though they exhibited parallel extinction; they are single crystals based on morphology. Also, note that 12 of the fragment's retardations were too low to observe extinction conditions.

The major difference between the Libby samples and the NIST tremolite is the larger number of "isotropic" particles in the former. For the Libby sample, the optical orientation, and thus extinction angle, differs from the tremolite samples. The extinction angle for the Libby samples is 20°, based on the single particle data in Table 8. Also, these samples have a lower retardation; thus, more "isotropic" particles occur. At first glance, it appears that more of the Libby fragments exhibit inclined extinction than the NIST samples. This would imply that more of the Libby particles rest on (110) than (100). However, this is probably not the case. Assuming that all the "isotropic" particles result from samples resting on (100), then for the NIST sample 29% of the particles rest on (110) and 67% on (100), and for the Libby samples 26% rest on (110) and 70% on (100).

DISCUSSION - SINGLE CRYSTALS

Observations from the photographs in Figures 2 and 3 reveal a trend in the size and shape of the three samples used in the study and the morphological characteristics of the fibers vs. fragments. Figures 2A and 2B show a UI tremolite sample viewed perpendicular to its widest dimension (Fig. 2A) and its thinnest direction (Fig. 2B). Clearly this is a single crystal (parallel sides, blunt ends), and its width to thickness ratio would be high when compared to the single crystal fragments of the NIST tremolite (Figs. 2G and 2H) and the Libby amphibole (Figs. 3G and 3H) viewed in similar orientations. The samples appear similar morphologically, the aspect ratios (l/w) are higher for the NIST and Libby samples, but the width to thickness aspect ratios appear lower. The remaining five sets of photographs are of fibers bundles and masses from the NIST tremolite (Figs. 2C to 2F) and the Libby amphibole (Figs. 3A to 3F). Differences in the morphology can be observed between these fiber bundles and single crystals. It is worth noting these particles were admixed in the deposits, i.e. they occurred together in the rock.

As seen in the photos of the fiber bundles in Figures 2 and 3, some of the samples appear more fibrous when viewed perpendicular to their widest direction (left column in Figures 2, 3). When the samples are rotated 90°, some of them appear much less fibrous (right column in Figures 2, 3). This is especially true in Figures 3D and 3F. A somewhat reverse observation for the NIST tremolite samples occurred. In Table 7, 11 of 25 samples had parallel extinction on the widest section, as would be the case if they were flattened on (100), as shown in Figure 4B. However, when rotated 90° the samples never went extinct, and although they appeared morphologically to be fragments (blunt end, parallel sides), they were fibers. Some of the NIST tremolite particles in grain mounts, that we classified as fragments, are probably fibers. This observation was only possible by rotating the samples and observing them in an orientation that would rarely be seen in a grain mount.

After these initial observations, our goal was to quantify the morphology so that we could calculate aspect ratios and measure extinction conditions for different orientations. The UI tremolite was used as a non-asbestos standard. We mounted 10 samples on a spindle stage in order to measure the thickest direction, corresponding to the width of the particle, and the thinnest direction, corresponding to the thickness of the particle (Table 6). The single crystals were rotated about the spindle axis until these directions were located. Data obtained in this manner are shown in Table 6A. These data show extinction angles that would be measured when the samples were viewed perpendicular, or near so, to (110) for all the samples except #4 and #10, which were viewed perpendicular to their (100) surfaces. The average value for extinction angles measured on the width is 14° which is nearly the same as was found in the grain mounts, 13°. Next, to measure the true extinction angle we repeated the measurements made in Table 6A, except each sample was rotated to place the (010) plane in the microscope stage, yielding an extinction angle of 16° (Table 6B). As was expected, in all cases these samples exhibited parallel extinction when (100) was in the plane of the microscope stage. Regardless of which table one uses, the aspect ratios increase significantly for l/t when compared to l/w.

an extinction angle of 13°, while one fragment rested on (100) and gave parallel extinction. For the NIST tremolite sample in Figure 1D (the circled crystal in 1C), the crystal shows inclined extinction indicating that the sample is resting on its (110) surface. Table 5 shows that 15 of the 99 NIST tremolite fragments were in this orientation, while 22 of them showed parallel extinction. Thus, 59% of the NIST fragments with observable extinction rested on (100), while 1% of the UI tremolite fragments were flattened on (100). These particles were fragments even though they exhibited parallel extinction; they are single crystals based on morphology. Also, note that 12 of the fragment's retardations were too low to observe extinction conditions.

The major difference between the Libby samples and the NIST tremolite is the larger number of "isotropic" particles in the former. For the Libby sample, the optical orientation, and thus extinction angle, differs from the tremolite samples. The extinction angle for the Libby samples is 20°, based on the single particle data in Table 8. Also, these samples have a lower retardation; thus, more "isotropic" particles occur. At first glance, it appears that more of the Libby fragments exhibit inclined extinction than the NIST samples. This would imply that more of the Libby particles rest on (110) than (100). However, this is probably not the case. Assuming that all the "isotropic" particles result from samples resting on (100), then for the NIST sample 29% of the particles rest on (110) and 67% on (100), and for the Libby samples 26% rest on (110) and 70% on (100).

DISCUSSION - SINGLE CRYSTALS

Observations from the photographs in Figures 2 and 3 reveal a trend in the size and shape of the three samples used in the study and the morphological characteristics of the fibers vs. fragments. Figures 2A and 2B show a UI tremolite sample viewed perpendicular to its widest dimension (Fig. 2A) and its thinnest direction (Fig. 2B). Clearly this is a single crystal (parallel sides, blunt ends), and its width to thickness ratio would be high when compared to the single crystal fragments of the NIST tremolite (Figs. 2G and 2H) and the Libby amphibole (Figs. 3G and 3H) viewed in similar orientations. The samples appear similar morphologically, the aspect ratios (l/w) are higher for the NIST and Libby samples, but the width to thickness aspect ratios appear lower. The remaining five sets of photographs are of fibers bundles and masses from the NIST tremolite (Figs. 2C to 2F) and the Libby amphibole (Figs. 3A to 3F). Differences in the morphology can be observed between these fiber bundles and single crystals. It is worth noting these particles were admixed in the deposits, i.e. they occurred together in the rock.

As seen in the photos of the fiber bundles in Figures 2 and 3, some of the samples appear more fibrous when viewed perpendicular to their widest direction (left column in Figures 2, 3). When the samples are rotated 90°, some of them appear much less fibrous (right column in Figures 2, 3). This is especially true in Figures 3D and 3F. A somewhat reverse observation for the NIST tremolite samples occurred. In Table 7, 11 of 25 samples had parallel extinction on the widest section, as would be the case if they were flattened on (100), as shown in Figure 4B. However, when rotated 90° the samples never went extinct, and although they appeared morphologically to be fragments (blunt end, parallel sides), they were fibers. Some of the NIST tremolite particles in grain mounts, that we classified as fragments, are probably fibers. This observation was only possible by rotating the samples and observing them in an orientation that would rarely be seen in a grain mount.

After these initial observations, our goal was to quantify the morphology so that we could calculate aspect ratios and measure extinction conditions for different orientations. The UI tremolite was used as a non-asbestos standard. We mounted 10 samples on a spindle stage in order to measure the thickest direction, corresponding to the width of the particle, and the thinnest direction, corresponding to the thickness of the particle (Table 6). The single crystals were rotated about the spindle axis until these directions were located. Data obtained in this manner are shown in Table 6A. These data show extinction angles that would be measured when the samples were viewed perpendicular, or near so, to (110) for all the samples except #4 and #10, which were viewed perpendicular to their (100) surfaces. The average value for extinction angles measured on the width is 14° which is nearly the same as was found in the grain mounts, 13°. Next, to measure the true extinction angle we repeated the measurements made in Table 6A, except each sample was rotated to place the (010) plane in the microscope stage, yielding an extinction angle of 16° (Table 6B). As was expected, in all cases these samples exhibited parallel extinction when (100) was in the plane of the microscope stage. Regardless of which table one uses, the aspect ratios increase significantly for l/t when compared to l/w.

Table 7 lists data for the 25 particles measured for the NIST tremolite. For the NIST tremolite, the 10 single crystals yielded an extinction of 16°, which differs from the value of 12° in Table 5 for the NIST samples in the grain mount. This is because all of the single crystal particles measured on the spindle stages were flattened on (100), and some of the grain mount samples were on (110). Eleven of the 15 fiber bundles in the NIST sample showed parallel extinction on their widest direction (i.e., how they would rest in a grain mount); this confirms the observations of Wylie (21). However, based on their morphology, we would classify these particles as fragments and explain the parallel extinction by the fact that they rested on (100). As stated above, we only classified these particles as fibers when we rotated them 90° and noted they never went extinct in that orientation. We could also observe a fibrous nature in this orientation that did not exist in the other orientation but only in crossed polars (particle #7, Table 7). The remaining 4 particles never went extinct in any orientation (for example, particle #5, Table 7).

Table 8 gives the individual measurements and observations for the 50 particles of the Libby amphibole vein sample. As was the case for the NIST samples, we classified the Libby samples as either fragments or fibers based on their morphology, but there were two types of fibers in this sample: fiber bundles (e.g., particle #7, Table 8, Figs. 3A and 3B) similar to those in the NIST sample and fiber masses (e.g., particle #18, Table 8, Figs. 3E and 3F). The fiber bundles tended to have parallel extinction regardless of the orientation (i.e., the setting of the spindle stage rotation), while the fiber masses had measurable extinction angles in both the widest and narrowest directions, but the angles do not correspond to any extinction angles. There possibly was a different mode of occurrence for the masses and the bundles; however, all of these particles came from the same sample and should have undergone similar conditions of formation. The fragments yielded an average extinction angle of 20°, which is similar to that obtained from the grain mounts, although there was considerable scatter in the grain mount data.

CONCLUSION

Five amphibole samples were characterized with polarized light microscopy and the spindle stage. They include three amphibole samples from the former vermiculite mine located in Libby, Montana that were collected by the author (MEG) in October, 1999 (Libby amphibole) together with a NIST tremolite-asbestos standard (NIST tremolite) and a non-asbestos tremolite from the University of Idaho teaching collection (UI tremolite). Amphiboles from all of the samples were characterized as standard grain mounts and as single particles using the polarized light microscope and the spindle stage.

The size and morphology were determined for approximately 1000 particles in the grain mounts. Also, the length, width and thickness for 85 single particles were measured with the assistance of the spindle stage. This includes fifty (50) single particles of the Libby amphibole, twenty-five (25) of the NIST tremolite, and ten (10) of the UI tremolite. In addition, extinction angles for different (hk0) planes were measured by adjusting the particles so their crystallographic c-axes were parallel to the rotation axis of the spindle and related to the observations in the grain mounts.

Based on the regulatory counting criteria of asbestos (i.e., an aspect ratio of 3:1 or higher), 95% of the Libby amphibole, 92% of the NIST tremolite, and 48% of the UI tremolite were asbestos. Based on morphology, 36% of the Libby amphibole, 19% of the NIST tremolite, and 0% of the UI tremolite were asbestos.

One of the main goals of this study was to better characterize the Libby samples; no doubt over the next several years many similar studies will be performed. However, to date, there is only one study of the samples at Libby, and it is not in the open literature but rather in an EPA report (36). The study found that 100% of the particles had an aspect ratio greater than 3:1, 88% greater than 10:1, and 52% greater than 20:1. Again, this compares well to our study in which we found 95% greater than 3:1, 73% greater than 10:1, and 49% greater than 20:1.

The application of the spindle stage also made it easier to distinguish between fibers and non-fibrous cleavage fragments. It was found that many of the NIST tremolite particles appearing as fragments in grain mounts appear as fibers upon rotation. Extinction angles were also determined for different (hk0) planes and these data were used to help interpret the observations made on the grain mounts. These observations showed that the non-asbestos samples mainly rested on their (110) surfaces, although the smaller of these were flattened on (100); the small fragments in the NIST tremolite and Libby amphibole were predominantly flattened on (100).

APPENDIX

Table 1. Size Distribution (By Particle) for UI Tremolite, NIST Tremolite, and Libby Amphibole as Determined from Grain Mounts with a PLM

Sample	Width(μm)	Length (μm)				
		0-10	11-20	21-50	51-100	>100
UI tremolite	0-1	0	0	0	0	0
(n=100)	1.1-2	0	0	0	0	0
	2.1-5	0	0	0	0	0
	5.1-10	0	0	1	0	0
	>10	0	0	0	0	99
NIST	0-1	3	0	0	0	0
(n=99)	1.1-2	4	2	6	2	1
	2.1-5	2	7	11	6	1
	5.1-10	1	4	4	9	12
	>10	0	1	3	8	12
Libby outcrop	0-1	0	1	2	2	1
(n=298)	1.1-2	2	5	29	34	12
	2.1-5	1	3	24	45	51
	5.1-10	0	0	7	20	51
	>10	0	0	0	1	7
Libby vein	0-1	21	33	29	12	4
(n=299)	1.1-2	14	19	15	22	16
	2.1-5	6	8	14	13	27
	5.1-10	1	0	9	3	17
	>10	0	1	5	6	4
Libby float	0-1	26	34	48	14	14
(n=300)	1.1-2	18	20	33	10	14
	2.1-5	10	7	9	2	5
	5.1-10	3	6	1	5	2
	>10	0	1	8	2	8

Table 2. Percent of Fibers, Fragments, and Not Classified in the UI Tremolite, NIST Tremolite, and Libby Amphibole Determined Morphologically and Grouped by Aspect Ratio (l/w)

Sample	Aspect Ratio	Fibers(%)	Fragments (%)	Not Classified (%)	Total (%)
UI tremolite	<3	0	52	0	52
	3-5	0	29	0	29
	6-10	0	15	0	15
	11-20	0	4	0	4
	21-50	0	0	0	0
	51-100	0	0	0	0
	>100	0	0	0	0
NIST tremolite	<3	0	7	1	8
	3-5	1	18	7	26
	6-10	3	7	9	19
	11-20	9	14	10	33
	21-50	4	5	1	10
	51-100	2	1	1	4
	>100	0	0	0	0
Libby outcrop	<3	0	0	0	0
	3-5	0	3	0	3
	6-10	2	7	2	11
	11-20	8	8	7	23
	21-50	17	14	12	43
	51-100	7	3	3	13
	>100	3	2	2	7
Libby vein	<3	0	5	0.4	5.4
	3-5	0.4	8	3	11.4
	6-10	1	8	7	16
	11-20	5.5	5	11	21.5
	21-50	12	6	8	26
	51-100	6	2	1	9
	>100	10	0.7	0	10.7
Libby float	<3	0	8	0.7	8.7
	3-5	0	6.5	4	10.5
	6-10	3	4	10	17
	11-20	6	7	11	24
	21-50	12	2	10	24
	51-100	7	0.4	0.7	8.1
	>100	7	0.7	0	7.7

Table 3. Percent of Fibers, Fragments, and Not Classified in the Three Libby Amphibole Samples Combined from Table 2, and Grouped by Aspect Ratio (l/w)

Aspect Ratio	Fibers (%)	Fragments (%)	Not Classified (%)
<3	0	4.3	0.3
3-5	0.1	5.8	2.3
6-10	2	6.3	6.3
11-20	6.5	7	10
21-50	13	7	10
51-100	7	1.8	1.6
>100	7	1.1	0.6

Table 4. Summary of Classification of Fibers, Fragments, and Not Classified for the UI Tremolite, NIST Tremolite, and Libby Amphibole Based on Aspect Ratio and Morphology

	Sample	Fibers (%)	Fragments (%)	Not Classified (%)
A. Aspect Ratio	UI tremolite	48	52	-
	NIST	92	8	-
	outcrop	100	0	-
	vein	95	5	-
	float	91	9	-
	total (Libby)	95	5	-
B. Morphology	UI tremolite	0	100	0
	NIST	19	52	29
	outcrop	37	37	26
	vein	35	35	30
	float	35	29	36
	total (Libby)	36	33	31

Table 5. Summary of Extinction Measurements for UI Tremolite, NIST Tremolite, and Libby Amphibole in Grain Mounts[1]

Sample	Parallel	Inclined	"Isotropic"	Cannot Measure	Total
UI tremolite					
fragments	1	99 / 13°(4)	0	0	100
NIST					
fibers	13	0	6	0	19
fragments	22	15 / 12°(5)	12	2	51
not classified	7	1	21	0	29
total	42	16	39	2	99
Libby					
fibers					
outcrop	45	0	61	1	107
vein	18	0	83	5	106
float	18	0	83	1	102
total	81	0	227	7	315
fragments					
outcrop	16	31 / 27°(13)	73	1	121
vein	2	30 / 21°(8)	67	2	101
float	5	21 / 20°(8)	55	8	89
total	23	82	195	11	311
not classified					
outcrop	11	2	45	12	70
vein	1	0	90	1	92
float	3	0	105	1	109
total	15	2	240	14	271

[1]Entries in the table represent the number of particles in each sample that have the characteristics listed in the column heading. "Isotropic" means the particle's retardation was too low to observe extinctions. "Cannot measure" means the particle never went extinct or had wavy extinction. Also in the inclined column is the average extinction angle with its standard deviation in parentheses.

Table 6. Morphological Measurements Obtained with the Aid of a Spindle for Ten Particles of the UI Tremolite Sample[1]

A. Width (w) and thickness (t) obtained from the widest and thinnest part of the sample; extinction angles (e.a. on w and e.a. on t) were obtained in these same orientations.

Particle	l (μm)	w (μm)	t (μm)	e.a. on w	e.a. on t	l/w	l/t	w/t
1	297	114	34	12°	15°	2.6	8.7	3.4
2	381	149	82	15°	16°	2.6	4.6	1.8
3	437	133	28	12°	17°	3.3	15.6	4.8
4	403	55	27	parallel	15°	7.3	14.9	2.0
5	667	127	98	14°	16°	5.3	6.8	1.3
6	134	96	73	16°	13°	1.4	1.8	1.3
7	442	59	32	16°	11°	7.5	13.8	1.8
8	567	146	106	11°	16°	3.9	5.3	1.4
9	562	120	38	13°	18°	4.7	14.8	3.2
10	852	76	50	parallel	15°	11.2	17.0	1.5

B. Width (w100) and thickness (t010) obtained on (100) and (010) planes; extinction angles (100 e.a. and 010 e.a.) were obtained in these same orientations.

Particle	l (μm)	w100 (μm)	t010 (μm)	100 e.a.	010 e.a.	l/w100	l/t010	w100/t010
1	297	104	42	parallel	17°	2.9	7.1	2.5
2	381	140	85	parallel	17°	2.7	4.5	1.6
3	437	123	71	parallel	17°	3.6	6.2	1.7
4	403	55	27	parallel	15°	7.3	14.9	2.0
5	667	103	93	parallel	14°	6.5	7.2	1.1
6	134	74	74	parallel	17°	1.8	1.8	1.0
7	442	33	44	parallel	16°	13.4	10.0	0.8
8	567	143	81	parallel	17°	4.0	7.0	1.8
9	562	113	32	parallel	16°	5.0	17.6	3.5
10	852	76	50	parallel	15°	11.2	17.0	1.5

[1]All ten particles were fragments based on morphology, while 7 of 10 would be classified as asbestos based on aspect ratio.

Table 7. Morphological Measurements Obtained with the Aid of a Spindle for Twenty-five Particles of the NIST Tremolite Sample[1]

Particle	l (μm)	w (μm)	t (μm)	l/w	l/t	w/t	e.a. on w	e.a. on t	type
1	493	83	54	6	9	1.5	parallel	never	fiber bundle
2	169	8	6	21	28	1.3	parallel	16°	fragment
3	744	88	40	8	19	2.2	parallel	never	fiber bundle
4	709	57	22	12	32	2.6	parallel	never	fiber bundle
5	728	175	78	4	9	2.2	never	never	fiber bundle
6	815	116	84	7	10	1.4	never	never	fiber bundle
7	594	78	39	8	15	2.0	parallel	never	fiber bundle
8	226	16	12	14	19	1.3	parallel	never	fiber bundle
9	435	29	15	15	29	1.9	parallel	17°	fragment
10	756	33	19	23	40	1.7	parallel	13°	fragment
11	1023	71	16	14	64	4.4	parallel	never	fiber bundle
12	644	40	29	16	22	1.4	parallel	never	fiber bundle
13	561	9	5	62	112	1.8	never	never	fiber bundle
14	630	95	67	7	9	1.4	never	never	fiber bundle
15	445	107	52	4	9	2.1	parallel	never	fiber bundle
16	146	32	21	5	7	1.5	parallel	never	fiber bundle
17	536	18	7	30	77	2.6	parallel	16°	fragment
18	875	27	20	32	44	1.4	parallel	16°	fragment
19	521	58	36	9	14	1.6	parallel	18°	fragment
20	473	42	28	11	17	1.5	parallel	17°	fragment
21	302	49	25	6	12	2.0	parallel	15°	fragment
22	602	39	14	15	43	2.8	parallel	never	fiber bundle
23	920	28	20	33	46	1.4	parallel	15°	fragment
24	718	48	18	15	40	2.7	parallel	17°	fragment
25	579	86	35	7	17	2.5	parallel	never	fiber bundle

[1]Width (w) and thickness (t) obtained from the widest and thinnest part of the sample; extinction angles (e.a. on w and e.a. on t) were obtained in these same orientations. Particle "type" determined based on morphological characteristics.

Table 8. Morphological Measurements Obtained with the Aid of a Spindle Stage for Fifty Particles of the Libby Vein Sample[1]

Particle	l (μm)	w (μm)	t (μm)	l/w	l/t	w/t	e.a. on w	e.a. on t	type
1	333	47	21	7	16	2.2	never	22°	fiber bundle
2	530	62	47	9	11	1.3	never	never	fiber mass
3	660	68	42	10	16	1.6	17°	22°	fiber bundle
4	577	122	67	5	9	1.8	parallel	parallel	fiber bundle
5	438	116	64	4	7	1.8	parallel	parallel	fiber bundle
6	654	60	32	11	20	1.9	parallel	parallel	fiber bundle
7	537	99	54	5	10	1.8	parallel	parallel	fiber bundle
8	362	83	63	4	6	1.3	10°	parallel	fiber mass
9	387	53	52	7	7	1.0	15°	10°	fiber bundle
10	321	46	28	7	11	1.6	parallel	19°	fragment
11	428	105	47	4	9	2.2	13°	parallel	fragment
12	492	78	58	6	8	1.3	parallel	parallel	fiber bundle
13	519	77	31	7	17	2.5	9°	parallel	fiber bundle
14	940	157	101	6	9	1.6	parallel	17°	fragment
15	1341	52	31	26	43	1.6	never	never	fiber bundle
16	354	180	162	2	2	1.1	39°	7°	fiber mass
17	541	105	61	5	9	1.7	parallel	parallel	fiber bundle
18	438	141	87	3	5	1.6	14°	13°	fiber mass
19	328	168	85	2	4	2.0	20°	parallel	fiber mass
20	700	73	69	10	10	1.1	parallel	parallel	fragment
21	392	142	66	3	6	2.2	10°	parallel	fragment
22	512	73	55	7	9	1.3	parallel	parallel	fiber bundle
23	316	52	38	6	8	1.4	parallel	parallel	fiber bundle
24	467	28	13	17	36	2.2	7°	parallel	fragment
25	714	73	29	10	25	2.5	parallel	19°	fragment
26	432	91	44	5	10	2.1	parallel	22°	fragment
27	423	70	56	6	8	1.3	22°	18°	fragment
28	591	74	38	8	16	1.9	15°	10°	fiber bundle
29	1460	71	36	21	41	2.0	never	never	fiber bundle
30	481	37	13	13	37	2.8	parallel	23°	fragment
31	764	142	111	5	7	1.3	never	never	fiber mass
32	661	45	28	15	24	1.6	parallel	21°	fragment
33	772	30	24	26	32	1.3	parallel	parallel	fiber bundle
34	542	53	39	10	14	1.4	parallel	parallel	fiber bundle
35	481	35	25	14	19	1.4	parallel	15°	fragment
36	627	57	48	11	13	1.2	20°	parallel	fiber bundle
37	483	26	12	19	40	2.2	parallel	23°	fragment
38	456	36	32	13	14	1.1	parallel	22°	fragment
39	587	29	23	20	26	1.3	parallel	parallel	fiber bundle
40	728	26	12	28	61	2.2	parallel	22°	fragment
41	738	140	103	5	7	1.4	12°	parallel	fiber bundle
42	363	89	81	4	4	1.1	parallel	parallel	fiber bundle
43	309	22	21	14	15	1.0	parallel	parallel	fiber bundle
44	546	74	40	7	14	1.9	parallel	23°	fragment
45	321	10	8	32	40	1.3	parallel	parallel	fiber bundle
46	327	50	44	7	7	1.1	parallel	21°	fragment
47	375	40	24	9	16	1.7	parallel	23°	fragment
48	710	50	34	14	21	1.5	parallel	parallel	fiber bundle
49	497	20	7	25	71	2.9	parallel	16°	fragment
50	703	17	17	41	41	1.0	27°	20°	fiber bundle

[1]Width (w) and thickness (t) obtained from the widest and thinnest part of the sample; extinction angles (e.a. on w and e.a on t) were obtained in these same orientations. Particle "type" determined based on morphological characteristics.

REFERENCES CITED

(1) Selikoff, I.J., Churg, J., and Hammond, E.C. "Asbestos exposure and neoplasia"; *Journal of the American Medical Association* **1984**, 252, 91-95.

(2) Skinner, H.C.W., Ross, M., and Frondel, C. *Asbestos and other fibrous materials; mineralogy, crystal chemistry, and health effects*; Oxford University Press: New York, 1988.

(3) Guthrie, G.D., Jr. and Mossman, B.T. eds. *Reviews in Mineralogy: Health effects of mineral dusts, 28*; Mineralogical Society of America, Washington, D.C. 1993.

(4) Nolan, R.P., Langer, A.M., Ross, M., Wicks, F.J., and Martin, R.F. *The health effects of chrysotile asbestos: contribution of science to risk-management decisions*; Special Publication #5, Mineralogical Association of Canada, Ottawa, 2001.

(5) Ross, M. "The geologic occurrences and health hazards of amphibole and serpentine asbestos"; In *Reviews in Mineralogy: Amphiboles and other hydrous pyriboles-mineralogy*; D.R. Veblen, Ed.; 1981; 9A, 279-323.

(6) Mossman, B.T., Bignon, J., Corn, M., Seaton, A., and Gee, J.B.L. "Asbestos: Scientific developments and implications for public policy"; *Science* **1990**, 247, 294-301.

(7) Gunter, M.E. "Asbestos as a metaphor for teaching risk perception"; *Journal of Geological Education* **1994**, 42, 17-24.

(8) Weill, H., Abraham, J.L., Balmes, J.R., Case, B., Chrug, A., Hughes, J., Schenker, M., and Sebastien, P. "Health effects of tremolite"; *American Review of Respiratory Diseases* **1990**, 142, 1453-1458.

(9) Case, B.W. "Health effects of tremolite"; In *The third wave of asbestos disease: Exposure to asbestos in place*; P.J. Landrigan, H. Kazemi, Eds.; Annals of the New York Academy of Sciences, 1991; 643, 491-504

(10) Nolan, R.P, Langer, A.M., Oechsle, G.W., Addison, J., and Colflesh, D.E. "Association of tremolite habit with biological potential: Preliminary report"; *In Mechanisms in fibre carcinogenesis*; R.C. Brow, J.A. Hoskins, N.F. Johnson, Eds.; 1991; 231-251.

(11) Davis, J.M.G., Addison, J., Bolton, R.E., Donaldson, K., Jones, A.D., and Miller, B.G. "Inhalation studies on the effects of tremolite and brucite dust in rats"; *Carcinogenesis* **1985**, 6, 667-674.

(12) Davis, J.M.G, Addison, J., McIntosh, C., Miller, B.G., and Niven, K. "Variations in the carcinogenicity of tremolite dust samples of differing morphology"; *In The third wave of asbestos disease: Exposure to asbestos in place*; P.J. Landrigan, H. Kazemi, Eds.; Annals of the New York Academy of Sciences, 1991; 643, 473-490.

(13) Bandli, B.R. and Gunter, M.E. " Identification and characterization of mineral and asbestos particles using the spindle stage and the scanning electron microscope: The Libby, Montana, U.S.A. amphibole-asbestos as an example"; *The Microscope* **2001**, 49, 191-199.

(14) Wylie, A.G. and Verkouteren, J.R. "Amphibole asbestos from Libby, Montana: Aspects of nomenclature"; *American Mineralogist* **2000**, 85, 1540-1542.

(15) Gunter, M.E., Dyar, M.D., Twamley, B., Foit, F.F., Jr., and Cornelius, S. "Crystal chemistry and crystal structure of amphibole and amphibole-asbestos from Libby, Montana, U.S.A."; *American Mineralogist* **2003**, 1944-1952.

(16) Wylie, A.G. "Relationship between the growth habit of asbestos and the dimensions of asbestos fibers"; *Mining Engineering* **1988**, 40, 1036-1040.

(17) Wagner, J.C., Chamberlain, M., Brown, R.C., Berry, G., Poley, F.D., Davies, R., and Griffiths, D.M. "Biological effects of tremolite"; *British Journal of Cancer* **1982**, 45, 352-360.

(18) Wylie, A.G., Shedd, K.B., and Taylor, M.E. "Measurement of the thickness of amphibole asbestos fibers with the scanning electron microscope and the transmission electron microscope"; In *Microbeam Analysis*; K. Heinrich, Ed., San Francisco Press, San Francisco, California 1982; 181-187.

(19) Langer, A.M., Nolan, R.P., and Addison, J. "Distinguishing between amphibole asbestos fibers and elongate cleavage fragments of their non-asbestos analogues"; In *Mechanisms in fibre carcinogenesis*; R.C. Brow, J.A. Hoskins, N.F. Johnson, Eds; 1991; 253-267.

(20) Zoltai, T. "Asbestiform and acicular mineral fragments"; In *Health hazards of asbestos exposure*; I.J. Selikoff and E.C. Hammond, Eds.; Annals of the New York Academy of Sciences, 1979; 330, 621-643.

(21) Wylie, A.G. "Optical properties of the fibrous amphiboles"; In *Health hazards of asbestos exposure*; I.J. Selikoff and E.C. Hammond, Eds.; Annals of the New York Academy of Sciences, 1979; 330, 611-619.

(22) Zoltai, T. and Wylie, A.G. "Definitions of asbestos-related mineralogical terminology"; In *Health hazards of asbestos exposure*; I.J. Selikoff, E.C. Hammond, Eds.; Annals of the New York Academy of Sciences ,1979; 330, 707-709.

(23) OSHA "Occupational exposure to asbestos, tremolite, anthophyllite, and actinolite"; *Federal Register* **1992**, 57, 24310.

(24) Zoltai, T. "Amphibole asbestos mineralogy"; In *Reviews in Mineralogy: Amphiboles and other hydrous pyriboles—mineralogy*; D.R. Veblen, Ed.; 1981; 9A, 237-278.

(25) Dorling, M. and Zussman, J. (1987) "Characteristics of asbestiform and non-asbestifrom calcic amphiboles"; *Lithos* **1987**, 20, 469-489.

(26) Veblen, D.R. and Wylie, A.G. "Mineralogy of amphiboles and 1:1 layer silicates"; In *Reviews in Mineralogy: Health effects of mineral dusts*; G.D. Guthrie, Jr., B.T. Mossman Eds.; 1993; 28, 61-138.

(27) Ross, M., Nolan, R.P., Langer, A.M., and Cooper, W.C. "Health effects of mineral dusts other than asbestos"; *In Reviews in Mineralogy: Health effects of mineral dusts*; G.D. Guthrie, Jr. and B.T. Mossman Eds.; 1993; 28, 361-409.

(28) Van Oss, C.J., Naim, J.O., Costanzo, P.M., Giese, R.F., Jr, Wu, W., and Sorling, A.F. "Impact of different asbestos species and other mineral particles on pulmonary pathogenesis"; *Clays and Clay Minerals* **1999**, 47, 697-707.

(29) Gunter, M.E. "Quartz – the most abundant mineral species in the earth's crust and a human carcinogen"; *Journal of Geoscience Education* **1999**, 47, 341-349.

(30) Guthrie, G.D., Jr. "Mineral properties and their contributions to particle toxicity"; *Environmental Health Perspectives* **1997**, 105, 1003-1011.

(31) Guthrie, G.D., Jr. "Mineralogical factors affect the biological activity of crystalline silica"; *Applications to Occupational Environmental Hygiene* **1995**, 10, 1126-1131.

(32) Guthrie, G.D., Jr. "Biological effects of inhaled minerals"; *American Mineralogist* **1992**, 77, 225-243.

(33) Wylie, A.G. and Huggins, C.W. "Characteristics of a potassian winchite-asbestos from the Allamoore Talc District, Texas"; *Canadian Mineralogist* **1980**, 18, 101-107.

(34) Gunter, M.E. and Twamley, B. "A new method to determine the optical orientation of biaxial minerals: A mathematical approach"; *Canadian Mineralogist* **2001**, 39, 1701-1711.

(35) Wylie, A.G. and Schweitzer, P. "The effects of sample preparation and measuring methods on the shape and shape characterization of mineral particles: The case of wollastonite"; *Environmental Research* **1982**, 27, 52-73.

(36) Atkinson, G.R., Rose, D., Thomas, K., Jones, D., Chatfield, E.J., and Going, J.E. "Collection, analysis and characterization of vermiculite samples for fiber content and asbestos contamination"; Reports to EPA 1982, Project 4901-A32, Contract No. 68-01-5915.

(37) Su, S.C. and Bloss, F.D. "Extinction angles for monoclinic amphiboles and pyroxenes: a cautionary note"; *American Mineralogist* **1984**, 69, 399-403.